IMPROVING MARS APPROACH NAVIGATION USING OPTICAL DATA

Brian Rush, Shyam Bhaskaran, and Stephen P. Synnott
Jet Propulsion Laboratory, California Institute of Technology

Abstract

An important objective of future Mars missions is to land with increasing accuracy at the surface, requiring precise targeting of the trajectory at entry. The approach navigation accuracies obtained with radio data can be improved with optical data, using satellite images against a star background to pinpoint the spacecraft's Mars-centered state. This paper presents covariance studies showing that these data can produce entry accuracies better than $0^{\circ}.1$ in flight-path angle and better than one km in position. Simulations validate these results, using a realistic Phobos model, and considering the effects on the solution of errors in the model that affect the appearance of Phobos.

1. INTRODUCTION

An important objective of future Mars missions is to land spacecraft to ever increasing accuracies on the surface of Mars. This requires precise entry and descent phases, which in turn depend on navigating the spacecraft during the approach phase as accurately as possible. The current navigation techniques used to accomplish this rely primarily upon earth-based Doppler and range measurements to determine the spacecraft's state. Deviations from the nominal trajectory are then computed and maneuvers are executed to get the spacecraft back on course. However, for some missions the accuracy achieved from earth-based radio data alone is insufficient.

Additional navigation methods and data types during the approach phase are thus required to obtain the goal of precision landing. One data type which can help to meet this requirement is optical navigation imaging. These data consist of images of Phobos and/or Deimos, taken against a star background, that are used to estimate the spacecraft's Mars-centered trajectory.

This paper presents the results of two analyses showing the results obtainable by the optical navigation procedure: (1) a covariance analysis showing that these data,

of-plane directions and several km in the downtrack direction. The center-finding biases in pixel and line were considered but not adjusted in the fit, with a-priori uncertainties taken to be 1% of the diameter of Phobos and 5% of the diameter of Deimos. A value of 0.1 pixels was assumed for the data noise. Table 1 summarizes the nominal values of those parameters most likely to affect the covariance results.

Additional runs were performed, varying filter settings and picture scheduling, to test the sensitivity of the results to these parameters. These changes are also summarized in Table 1.

Table 1: Nominal and Alternative Settings for the Covariance Analysis

Parameter	Nominal Setting	Alternative Setting
Estimated Spacecraft State	APCOV resulting from radio covariance analysis	APSIGs of 50km and 100 cm/s in *each* X,Y,Z
Estimated Satellite Ephemerides	APCOV = 1 x covariance matrix	APCOV = 3 x cov. matrix
Considered Center-finding biases	APSIG = 1% & 5% of Phobos & Deimos diameter (approx. 110 m & 310 m, respectively)	APSIG = 3% & 15%
Data Noise	0.1 pixels in both pixel and line	0.3 pixels
Satellites imaged	Deimos & Phobos	Phobos only
Picture Frequency	Frequent (as noted in text)	6 x less frequent

APCOV = a-priori covariance (correlated matrix; see text for more details)
APSIG = a-priori standard deviation (uncorrelated)

The results of this covariance analysis are shown in figures 1–4. Figure 1 shows the 1-σ uncertainty in flight-path angle (FPA[1]), based on the complete consider analysis (i.e., including the effects of all estimated and considered parameters), plotted from 15 days to 1.5 days before entry[2]. Figure 2 shows these same data plotted from 36 hours to 12 hours before entry.

The lower line with squares on the data points represents the nominal case. The lines with various symbols represent those case where one of the alternative settings is applied, and other values are kept nominal. The upper line with squares is the

[1]FPA is the angle between the spacecraft trajectory the atmosphere at entry, measured outward from the tangent, i.e. just skimming the atmosphere is equivalent of an FPA of 0 degrees. The nominal value for the trajectory used for the calculations in this paper is -13°.00.

[2]The FPA uncertainty can also be used to estimate the uncertainty in "B-vector" magnitude, a parameter often used to describe approach trajectories. The B-vector approximates where the point of closest approach would be if the target planet had no mass and did not deflect the spacecraft. It lies in the "B-plane", with the origin at the center of Mars and perpendicular to the incoming spacecraft asymptotic velocity vector. $\sigma_{|B|}$ is a constant multiple of σ_{FPA} at all times for a given trajectory, in this case the ratio being 28.3 km/deg.

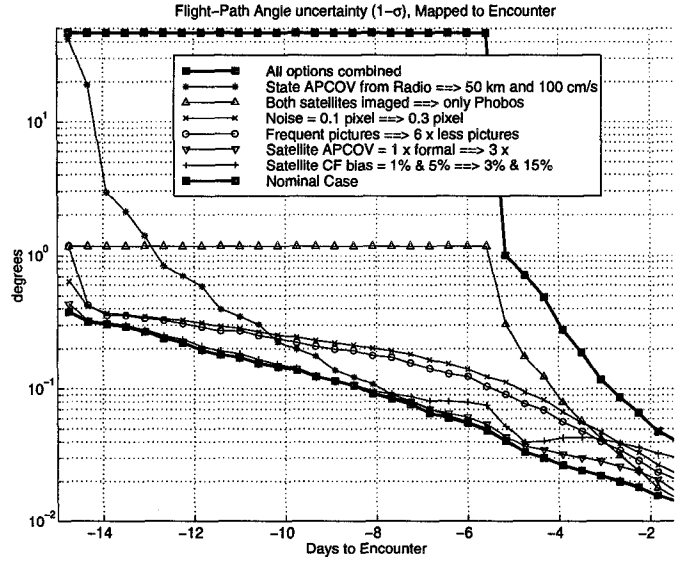

Figure 1: The 1-σ standard deviation of fligh-path angle, plotted from 15 days to 1.5 days before encounter.

case where all of the alternative settings are applied simultaneously, representing a worst-case scenario. In this case, the FPA uncertainty is under $0^\circ.03$ by the data cutoff at 12 hours before entry. Even at 24 hours before entry, the 3-σ uncertainty in FPA is below $0^\circ.1$, the lowest value quoted as a requirement by mission designers.

Figures 3 and 4 plot the semi-major axis (SMAA) of the 1-σ B-plane error ellipse, mapped to entry, spanning the same times and showing the same cases as figures 1 and 2, respectively. In the worst case, the 1-σ SMAA is under 1 km by 30 hours before entry, and decreases to 0.73 km by the 12-hour data cutoff. In the nominal case, the 1-σ SMAA is 0.26 km by 12-hours before entry. For the individual cases, each line shows the same general characteristics as with FPA uncertainty, and the discussion above also applies.

Looking at the changes resulting from varying settings individually, we see the following:

- First, we degraded the a-priori knowledge of the spacecraft state, using uncorrelated standard deviations of 50 km for position and 100 cm/s for velocity in each X,Y,Z direction. This approximates the case where the a-priori knowledge has not been improved by recent radio observations. This results in a greatly increased σ_{FPA} at first, but within a few days this case quickly approaches the nominal case, as the information obtained from the optical data

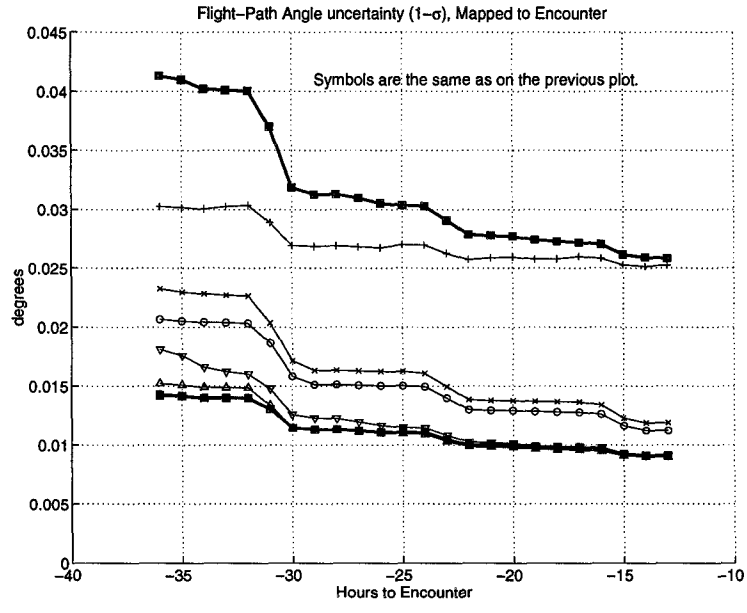

Figure 2: The 1-σ standard deviation of fligh-path angle, plotted from 36 hours to 12 hours before encounter.

contributes much more to the solution than the radio observations.

- Omitting observations of Deimos, σ_{FPA} remains at it's initial value until Phobos imaging begins, at which time it approaches the nominal case within a couple days, indicating that the Phobos observations contribute substantially more to the result than the Deimos observations.

  Although these first two cases (increased a-priori knowledge of state and omitting Deimos observations) show the greatest effect on σ_{FPA} early, by the last day before entry these two cases have the least effect.

- Increasing the a-priori covariance on the Phobos and Deimos ephemerides has a small, but noticeable effect early on, but the effect is less than $0^{\circ}.001$ by 24 hours before entry and completely negligible by 12 hours out. Increasing the satellite covariance by even a factor of 10 has a slightly greater, but similar effect, and also results in σ_{FPA} only slightly greater than the nominal case by 24 hours before entry.

- Decreasing picture frequency is one input that noticeably affects the results to the very end. Decreasing the picture frequency uniformly by a factor of 6 (i.e. Deimos imaging every 4 hours, then Phobos imaging every 1 hour until 36 hours before entry and every 12 minutes from the to 12 hours out) increases σ_{FPA} by 50–30% over the last 36–12 hours before entry.

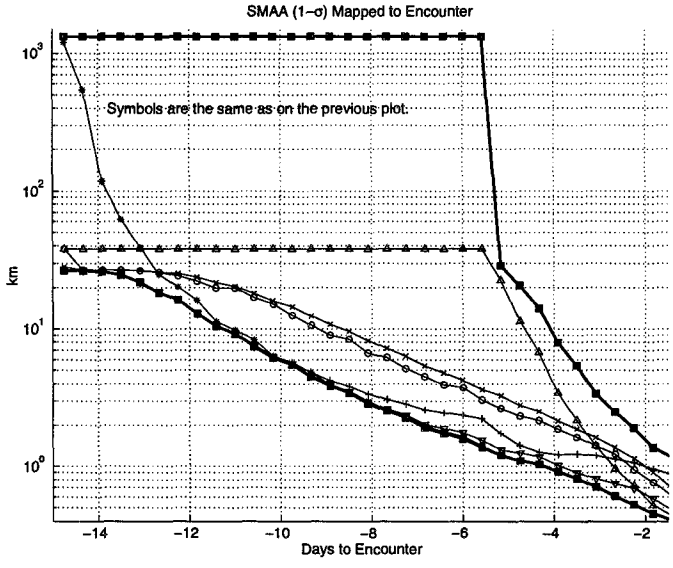

Figure 3: The semi-major axis of the 1-σ position error ellipse, plotted from 15 days to 1.5 days before encounter.

- Slightly greater effects are found by increasing the data noise to 0.3 pixels. This change increases σ_{FPA} by about 70–40% over the last 36–12 hours before entry.

- The greatest effect was found by increasing the center-finding biases – the values representing how well the center-of-figure of Phobos and Deimos as determined from the images represents the true line-of-sight to the center-of-mass of these objects. Increasing this value by a factor of 3 causes σ_{FPA} to be more than double the nominal case at 36 hours out, and then to level out by 12 hours before entry. By that time, almost the entire increase in σ_{FPA} in the worst case over the nominal case is caused by this factor.

  Thus, being able to accurately find the true center of the observed satellite from the optical image is a critical factor in minimizing the uncertainties in spacecraft state or FPA at atmospheric entry. The next section will describe how image modelling is used to determine this accurately, as well as tests done to verify the accuracy of this modelling.

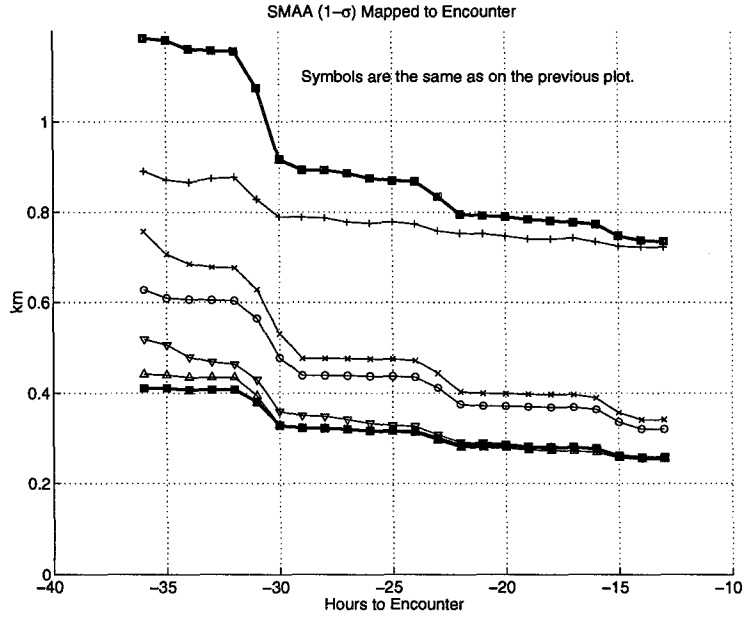

Figure 4: The semi-major axis of the 1-σ position error ellipse, plotted from 36 hours to 12 hours before encounter.

3. IMAGE SIMULATIONS

In flight, the opnav camera will take a picture at each scheduled time, and the pixel and line locations of the centroid of the satellite and background stars will be recorded. The pointing direction of the camera then is determined from the star images and is used to determine center-of-brightness ("CB") of each satellite image. The satellite locations comprise the observational data that are input to the dynamic filter. However, corrections must first be applied to these CB values, to account for the fact that they do not represent the center-of-mass ("CM") described by the satellite ephemerides and used in orbit determination.

The offset between CB and CM is described by two factors. First, the CB is offset from the center-of-figure ("CF"), which is the geometric image centroid, i.e. the centroid that would result if the satellite were uniformly illuminated. The CF is then offset from CM by the fact that satellite does not have a homogeneous mass distribution. The CB→CF offset can be corrected for if we know how the satellite will appear in a 2-D projection, including the affects of solar illumination from the proper direction. The CF→CM is more difficult to account for and is modelled as a systematic bias with a-priori values expressed as a percentage of the mean diameter of the object. This is currently accounted for by the center-finding bias described

taken in tandem with Doppler and range data, are capable of producing flight-path angle accuracies of better than 0°.1 and positional accuracies of better than 1 km at entry; and (2) simulations of the approach trajectory using a series of Phobos images, made with a realistic model, that validate the covariance results. These simulations also incorporate errors in the shape and orientation of Phobos, to test the effects of unmodelled errors on the solution.

The approach trajectory and camera parameters used in this case are those for the 2007 Mars Smart Lander, but the methods described herein are applicable to any Mars orbiter or lander mission.

2. COVARIANCE ANALYSIS

In order to assess the theoretical capabilities of the optical navigation system to improve the approach navigation accuracies, a covariance analysis was performed spanning the last couple weeks before the entry date of 07 September 2008. The trajectory was initialized 15 days before atmospheric entry, and the initial state uncertainty was constrained to match knowledge gained from earth-based Doppler and range data.

A schedule of images was generated, containing predicted pixel and line locations of the targets. Pictures were simulated for Deimos every 40 minutes, from 15 days to 5.5 days before atmospheric entry, and for Phobos every 10 minutes from 5.5 days to 1.5 days before entry and then every 2 minutes from 1.5 days to 12 hours before entry. The 12-hour cutoff is sufficient to allow the data to be downloaded and processed on the ground, and then for a trajectory-correction maneuver to be determined and uploaded to the spacecraft. Pictures where the satellite would be eclipsed or occulted by Mars, in transit to Mars, or too close to the edge of Mars to be clearly separated were omitted. A total of 801 pictures of Phobos and 223 pictures of Deimos were then used. This picture schedule was then used to calculate variational partials of the observed pixel and line values with respect to the state variables. These data were filtered using a batch-sequential least-squares filter to obtain the spacecraft-state uncertainties at epoch, which were mapped to the encounter conditions.

Parameters estimated in the fit were the spacecraft epoch state and the Phobos and Deimos ephemerides. Knowledge of the spacecraft state was constrained by an a-priori covariance matrix, representing the correlated uncertainties in position and velocity determined by ground-based radio observations. The corresponding 1-σ standard deviations are $\sim$64 km in position and $\sim$9 cm/s in velocity. The satellite ephemerides were constrained by their covariance based on ground observations. The corresponding standard deviations are several hundred meters in the radial and out-

above in the section on covariance analysis. Future analysis will account for this factor explicitly, as a vector that is defined in the model that is input to the filter.

To determine the CB→CF offset, realistic images of Phobos are generated using a 25,000-point model of the surface of Phobos, based on the latest topography and albedo information, projected into a 2-D image as would be seen by the camera. Figure 5 shows two images made using this method. The image on the left uses 1.4 μrad/pix resolution to show the model detail. The image on the right uses 22.9 μrad/pix resolution, convolved with a 2-D Gaussian point spread of $\sigma = 0.43$ pixels, to represent the opnav cameras being developed for the 2005 and 2007 Mars missions. We assume that the pointing direction of the camera has been determined to 0.1 pixels or better from the star images. Currently we are assuming no other error sources such as shot noise or detector read or dark-current noise. We are assuming that these will cause random errors that will be averaged out with the large number of frames that are acquired.

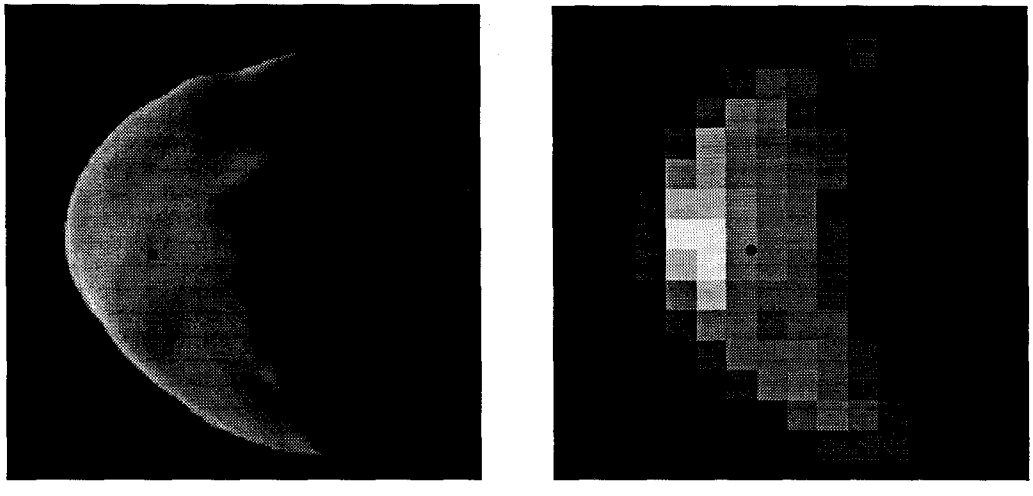

Figure 5: Two simulated images of Phobos, 5 hours before encounter, generated using a 25,000-vector model. The image on the left uses 1.4μrad/pix resolution to show the model detail. The image on the right uses 22.9μrad/pix resolution to represent the opnav cameras being developed for the 2005 and 2007 Mars missions. Phobos' solar phase is 108°.8.

For the current pre-flight analysis, *both* "truth" and "nominal" images are generated at each scheduled time using the vector model of Phobos. The truth images simulate the actual pictures that will be taken by the spacecraft during the mission, to be used to generate the observed pixel and line locations. The nominal images represent the images that will simulated during the mission, and are used to generate the *correction factors* that will be applied to the pixel and line locations

to retrieve the supposed location of the CF of Phobos. This CB→CF correction can then be applied to the CB of the "truth" image taken by the spacecraft before calculating residuals[3]. The importance of applying this correction is demonstrated in figures 6– 8.

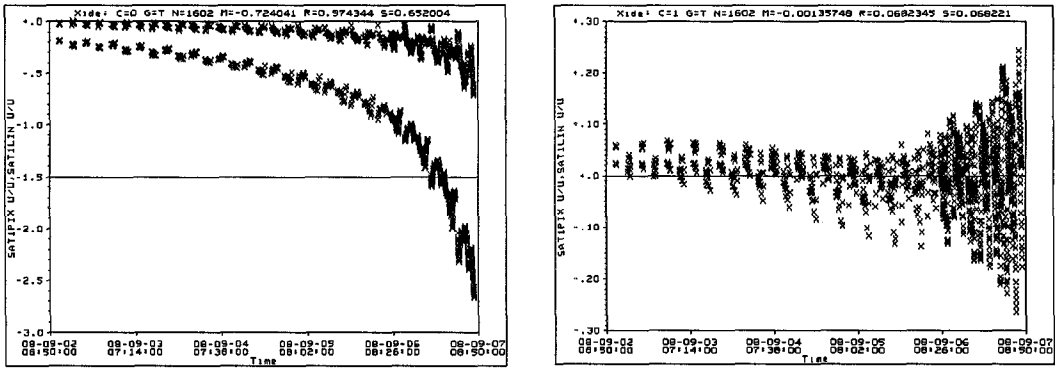

Figure 6: Pre-fit (left) and Post-fit (right) residuals without applying any CB→CF correction.

Figure 6 shows the pre- and post-fit residuals in pixel and line measurements, in the case where the CB→CF offset is not applied at all. With perfect modelling, there would be no systematic errors, and small residuals representing noise would be centered around zero. However, the large difference between CB and CF in this case results in significant and systematic pre-fit residuals. The post-fit residuals are smaller, but the filter cannot completely remove the signature of the offset, and tries to compensate by changing the values of the spacecraft state. The result is entry-state errors of over 20 km in position and 0°.3 in FPA. These unacceptable results demonstrate that a CB→CF correction must be applied.

Figure 7 shows the pre- and post-fit residuals in the case where a CB→CF correction *is* applied, by assuming a spherical model of Phobos illuminated by the Sun from the correct phase angle. In this case, the simplified correction improves the pre-fit residuals by an order of magnitude, but the post-fit residuals are only marginally better than the case with no correction. The result is that the solution still has entry-state errors, of 2.5 km in position and 0°.03 in flight-path angle. These errors are above the 3-σ values determined by the nominal covariance analysis (and the 1-σ values of the worst-case case), and this is *without* including the effects of state errors or observational errors.

This highlights the fact that it is critical to apply an accurate CB→CF correction

[3]In optical navigation, residual plots represent the difference between observed and predicted pixel and line values of the image centroid, as a function of time

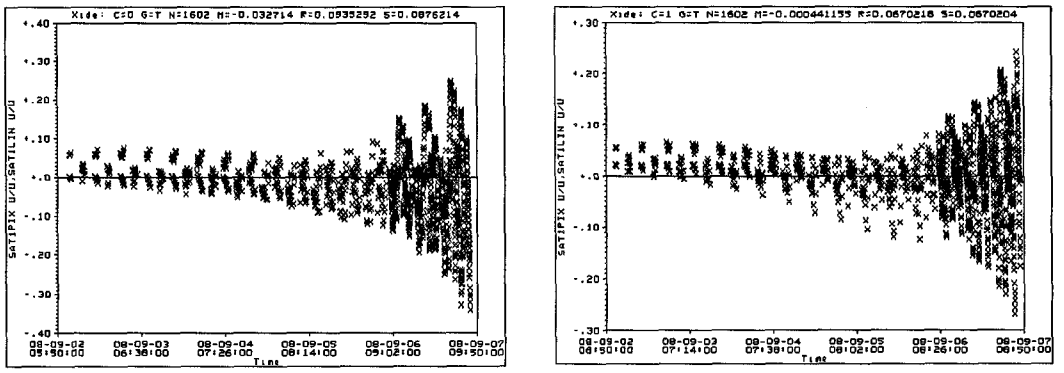

Figure 7: Pre-fit (left) and Post-fit (right) residuals after applying an CB→CF correction assuming a spherical model of Phobos.

based on our detailed model of Phobos in order to obtain accurate optical navigation during Mars approach. To test the sufficiency of this model, and to account for any possible modelling errors, we have run several cases, intentionally introducing errors into our nominal image set, by rotating, tilting, or precessing Phobos or by scaling its size, thus changing the appearance of Phobos as seen from the spacecraft. Once these images are generated, the imperfectly-corrected set of observations are sent to the filter for processing. The filter is then used to obtain a trajectory solution which can be compared to the known truth trajectory. The specific modelling errors introduced are not fit by the filter explicitly, and therefore cannot be corrected for directly, resulting in errors in the spacecraft state. This represents a worst-case scenario in which unmodellable (or unknown) error sources degrade the solution. A set of such solutions was analyzed, to investigate the effects of these errors.

Figure 8 shows the residuals that result from the case in which we rotate Phobos 2°.0 from it's nominal orientation (a value significantly greater than the uncertainty in the rotational state of Phobos; similar results were found when introducing other errors into the Phobos model). As expected, the residuals increase with time, as the angular size of Phobos as seen from the spacecraft increases. However, the magnitude of these residuals is less than the those resulting from the uncorrected or spherically-corrected images discussed above. These residuals are also symmetric around zero, roughly equivalent to adding noise to the images, as opposed to displaying a systematic trend as in the above cases. The result is that less of an error is introduced into the spacecraft state. In this case, the errors mapped to atmospheric entry are 0°.0023 in FPA, and 0.063 km parallel to the semi-major axis of the position error ellipse. Compared to the results of the covariance analysis, these are 0.25-σ values, even of the nominal case with data taken to 12 hours before encounter. These preliminary results indicate that unmodellable errors sources in

the appearance of Phobos degrade the solution by factors significantly smaller than the uncertainties obtained by the covariance analysis.

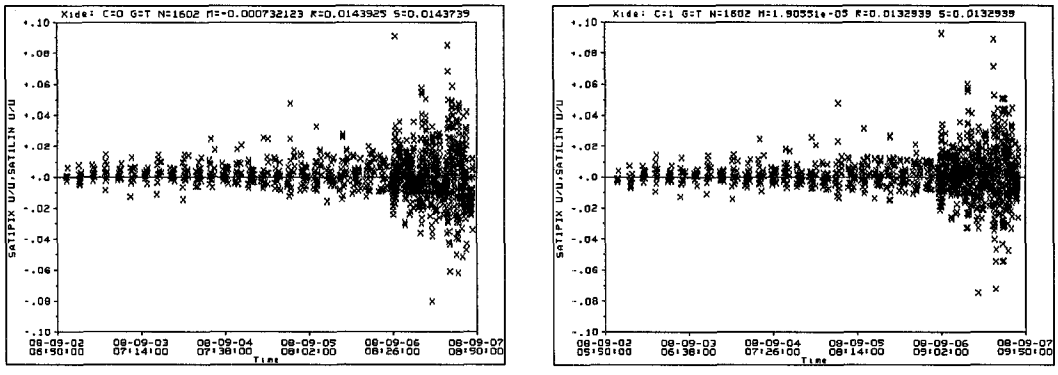

Figure 8: Pre-fit (left) and Post-fit (right) residuals after center-of-brightness to center-of-figure corrections have been made using a simulated image of Phobos, with a 2°.0 rotational error incorporated into the model.

3. SUMMARY AND CONCLUSIONS

A covariance analysis has been performed to show the contribution that optical navigation techniques can make to improving Mars approach navigation. Given a nominal set of assumptions, and taking observations until 12 hours before entry, the 3-σ FPA uncertainty mapped to atmospheric entry is less than 0°.03. Increasing the assumed a-priori uncertainty in the spacecraft and/or satellite ephemerides, or omitting Deimos and restricting observations to Phobos, have very little effect on the covariance results. Decreasing the frequency of observations or increasing data noise have small but noticeable effects. The greatest increase in FPA uncertainty was obtained by increasing the center-finding bias. But even given the pessimistic assumption of combining all of these factors, the 3-σ uncertainty in the FPA, mapped to atmospheric entry, is below 0°.1 (the requirement imposed by mission designers) as early as 24 hours before entry.

A detailed model of Phobos has been developed that is used to simulate the optical navigation images taken in-flight. This is necessary in order to determine the offset between the center-of-brightness of the images and the geometric center-of-figure of Phobos from the point of view of the spacecraft. Making such a correction is critical, as indicated by simulations showing the severe entry-state errors that result when this CB→CF correction is *not* applied, and smaller, but still significant errors that result when a simplified correction is applied. The affect of unmodelled or unknown errors affecting the modelled appearance of Phobos will not degrade

the solution, as further tests show that such modelling errors introduce state errors much smaller than the covariance results.

Future tests to validate the covariance results will include simulations that mimic additional errors sources which might occur in flight, but which are not modelled in covariance studies, including errors in the orbital dynamics and position of Phobos. The CF→CM offset will also be accounted for explicitly, as a vector that is defined in the model that is input to the filter. Monte-Carlo simulations will also be performed to test the effect on the solution of a wide range of possible spacecraft state errors. The ability of the dynamic filter to recover the entry state position and fligh-path angle in the presence of such errors will be compared to the uncertainties expected by the covariance analysis. Further, it will be verified that shot noise and detector noise are easily averaged out.

We thank R. Gaskell for providing the 3-D model of Phobos, and software for rendering 2-D projections, as used in the imaging simulations.

The research described in this paper was carried out at the Jet Propulsion Laboratory, California Institute of Technology, under a contract with the National Aeronautics and Space Administration.

Mars Relative View

2008/09/07 16:57:00.00

.Mars CI Observer, .Mars Pointing, [km min rad]+

1.21

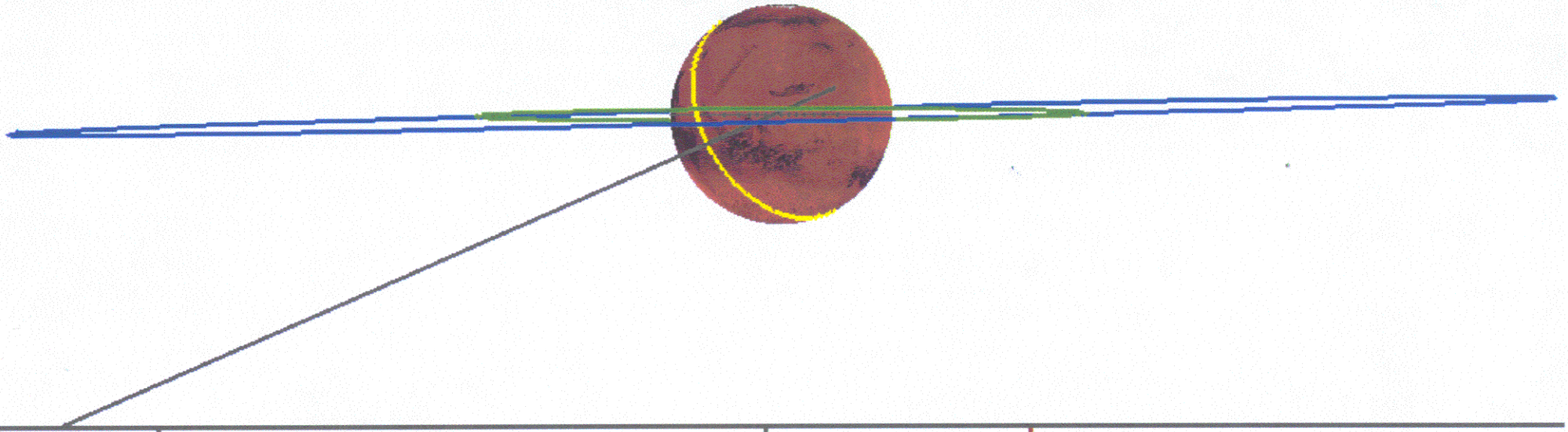

Mars Relative View3

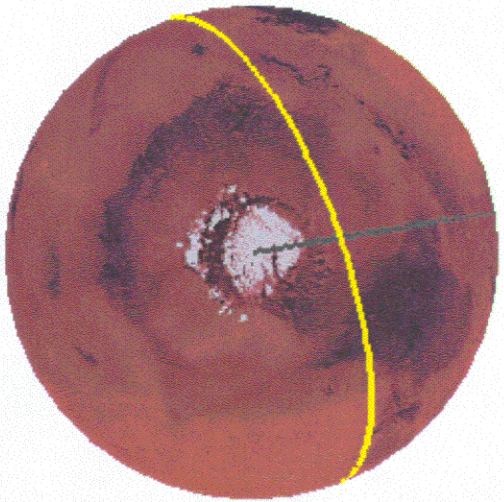

Mars Relative View2

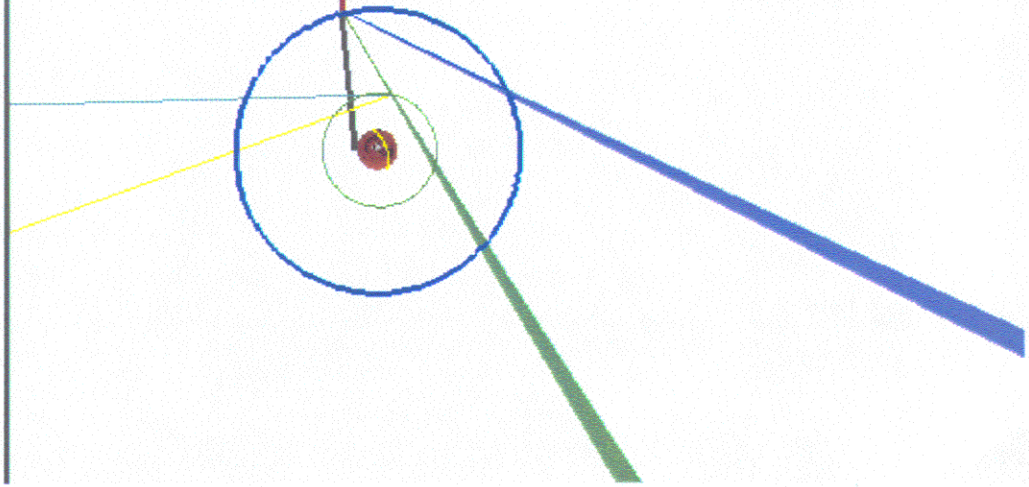

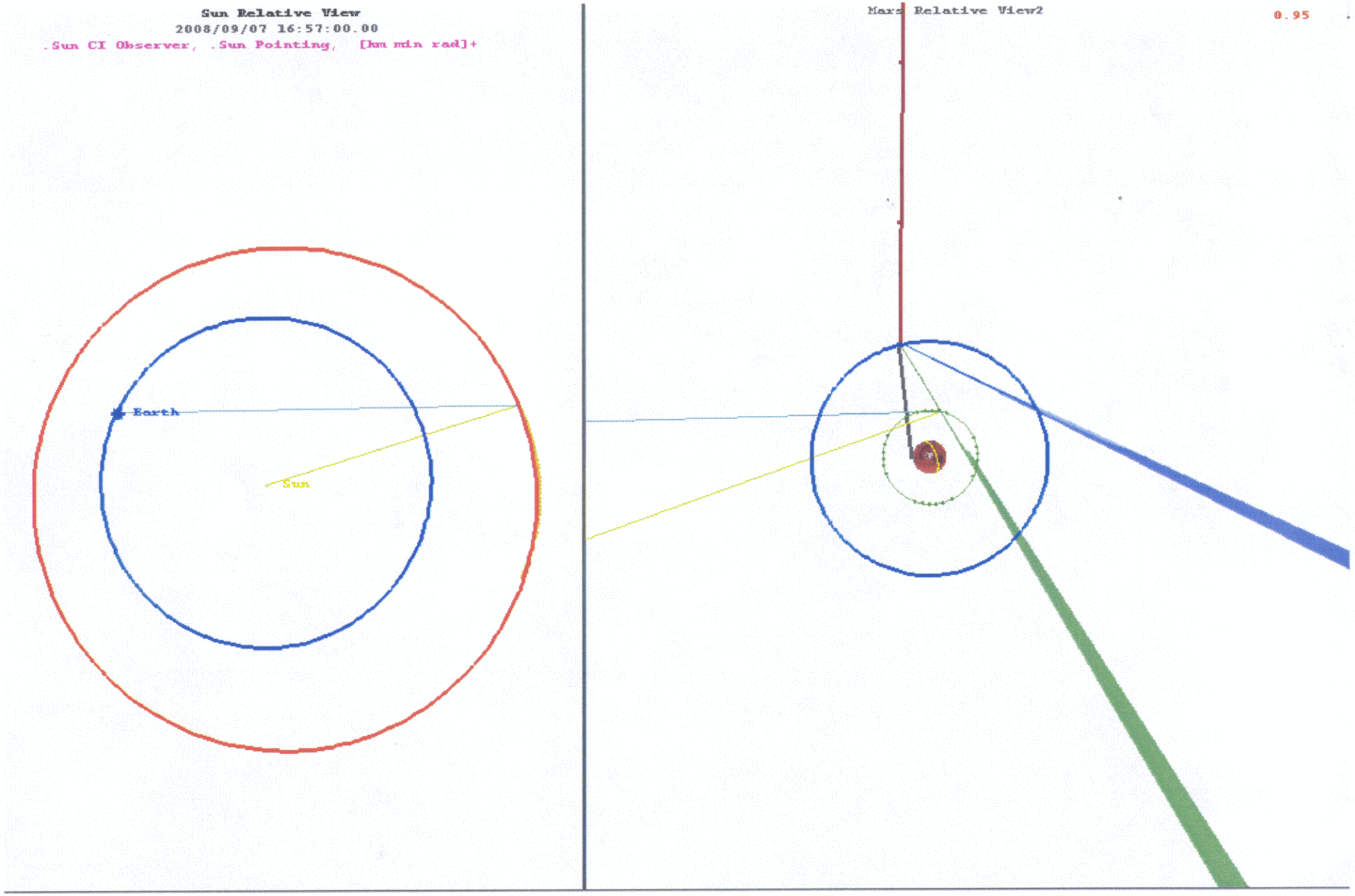
Sun Relative View
2008/09/07 16:57:00.00
.Sun CI Observer, .Sun Pointing, [km min rad]+
Earth
Sun
Mars Relative View2
0.95

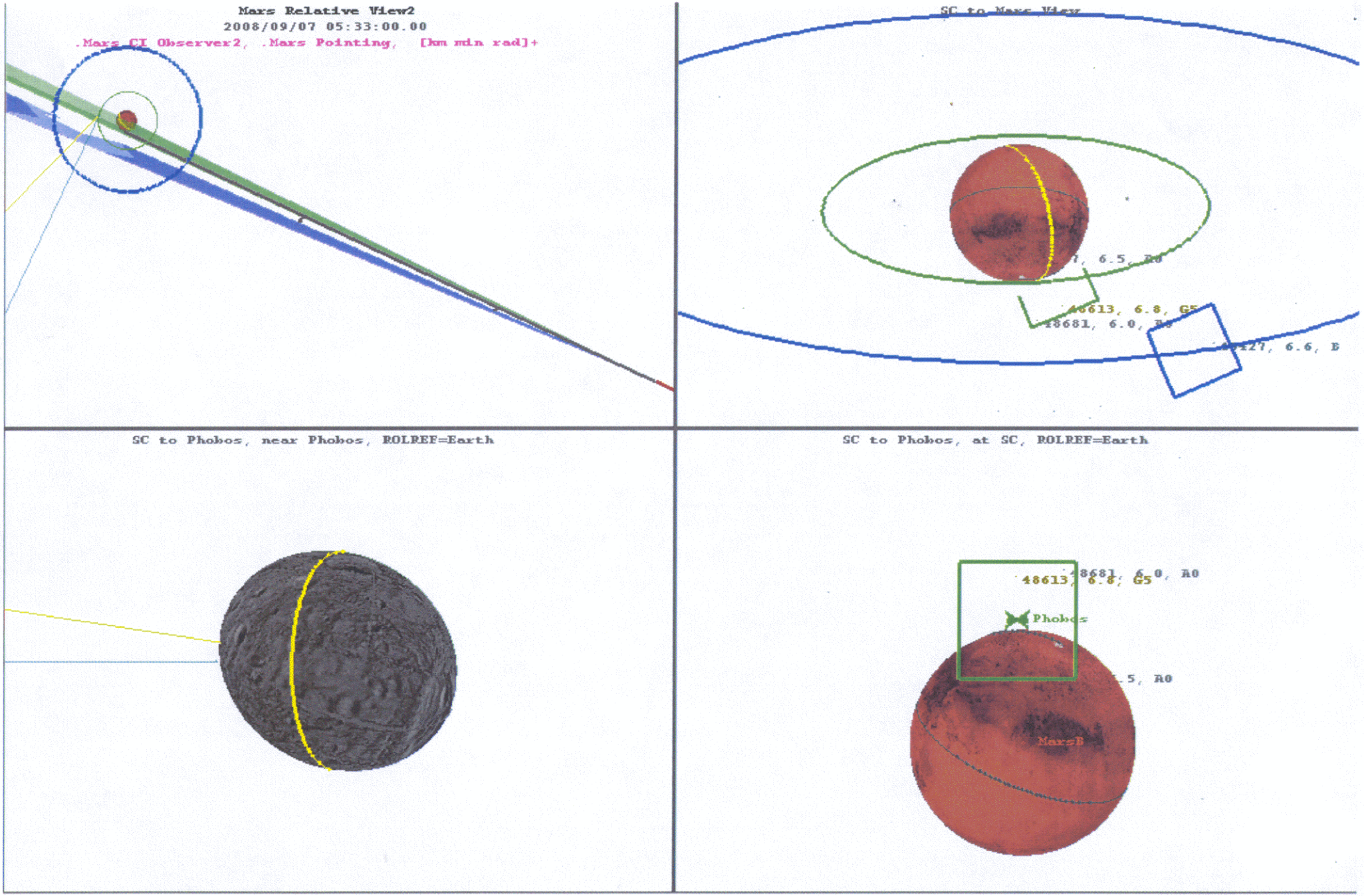
Mars Relative View2
2008/09/07 05:33:00.00
.Mars CI Observer2, .Mars Pointing, [km min rad]+
SC to Mars View
48613, 6.8, G5
48681, 6.0, A0
SC to Phobos, near Phobos, ROLREF=Earth
SC to Phobos, at SC, ROLREF=Earth
48613, 6.8, G5
Phobos
MarsB

B-PLANE COORDINATE SYSTEM

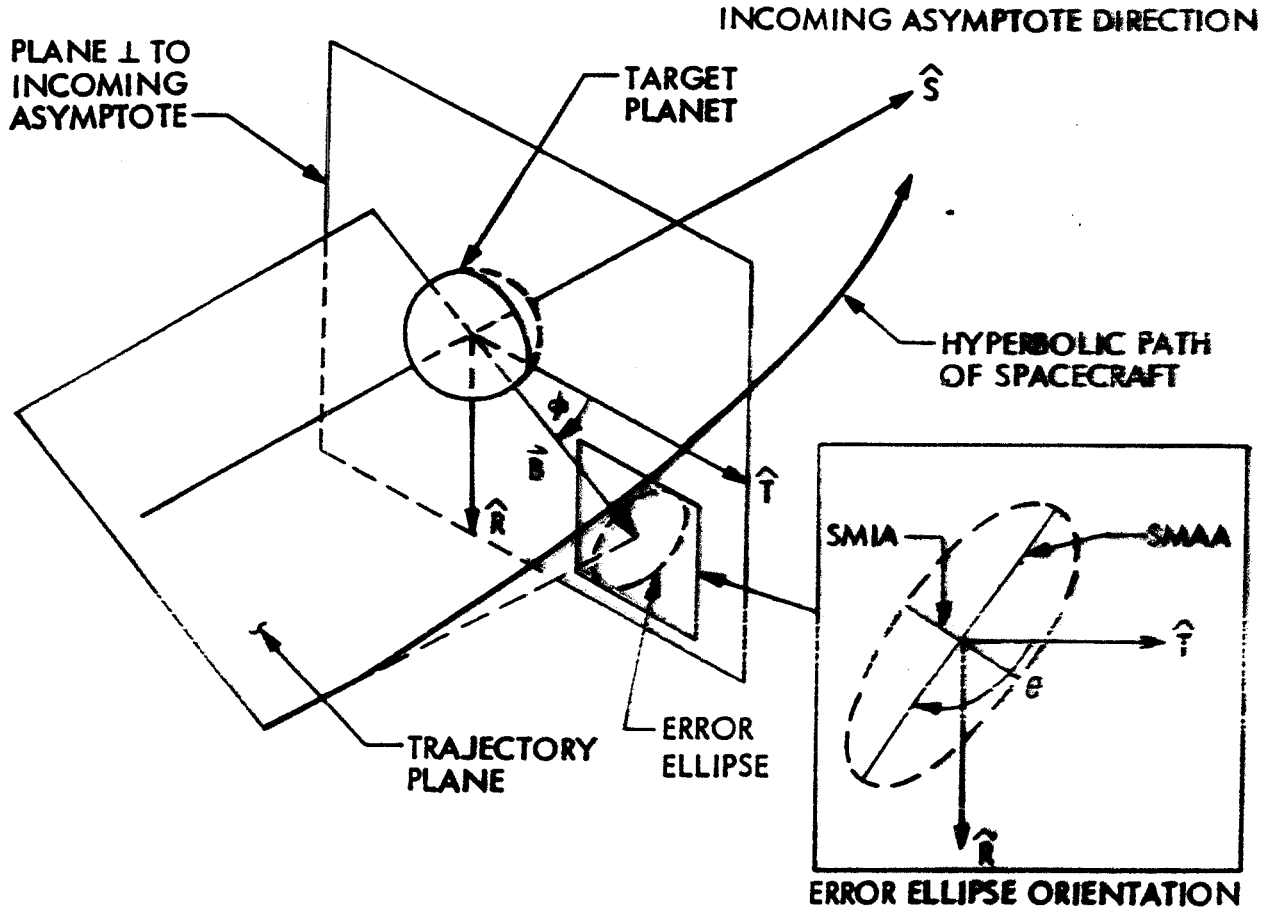

$\vec{B}$ = MISS PARAMETER = $\frac{1}{V_\infty}(\hat{S} \times \vec{H})$, i.e., $\vec{B} \times (V_\infty \hat{S}) = \vec{H}$

$\vec{H}$ = ANGULAR MOMENTUM VECTOR

$H = BV_\infty$

V_∞ = VELOCITY AT INFINITY

$\hat{T}$ = PARALLEL TO ECLIPTIC PLANE AND NORMAL TO $\hat{S}$

$\hat{R} = \hat{S} \times \hat{T}$

Flight Path Angle

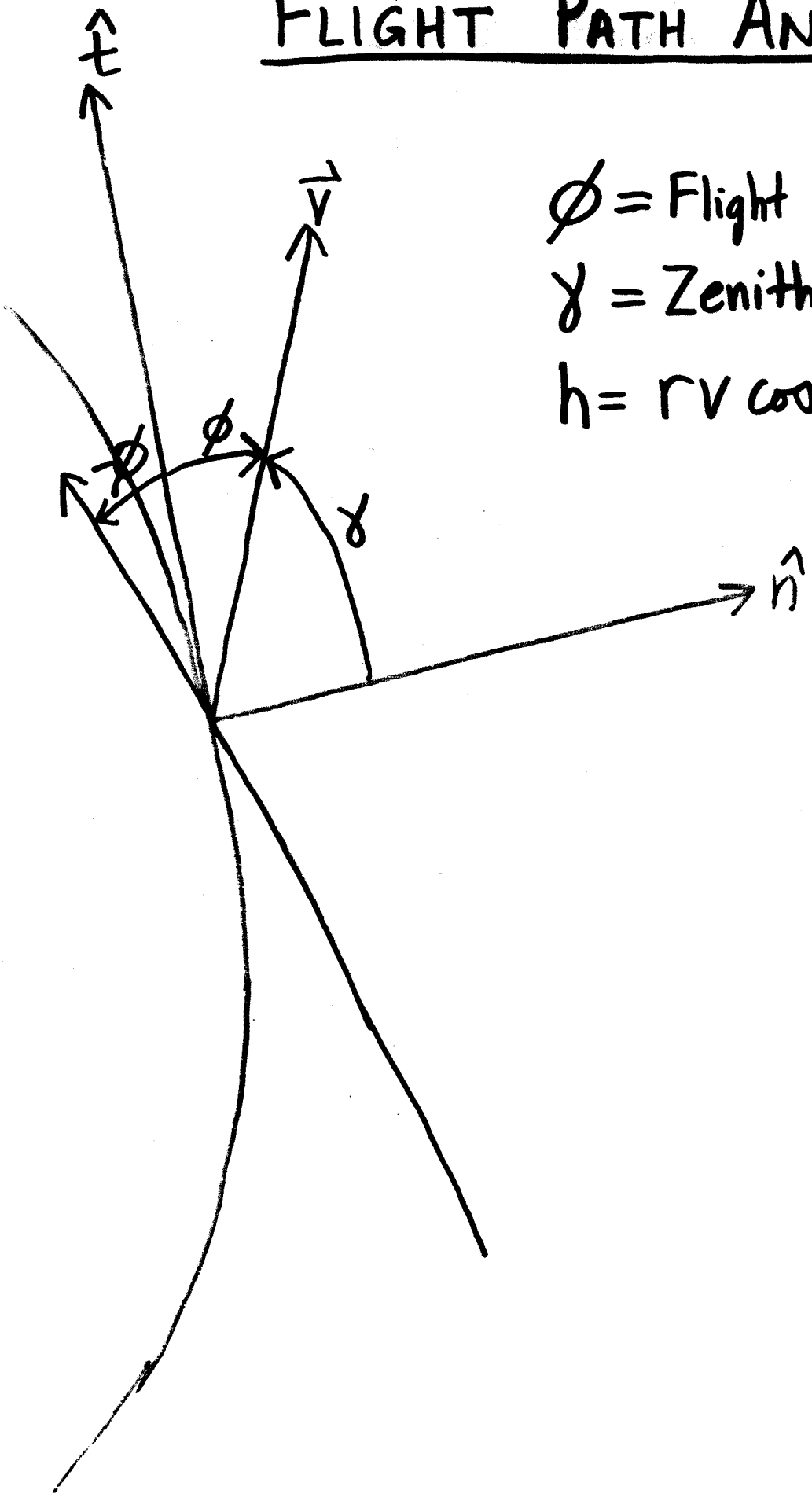

ϕ = Flight Path Angle

γ = Zenith Angle

$h = rv\cos\phi$

$$h = rV\cos\phi$$

$$h = BV_\infty$$

$$B = r\frac{V}{V_\infty}\cos\phi$$

$$\frac{\delta B}{B} = \frac{\delta r}{r} + \left[\frac{\delta V}{V} - \frac{\delta V_\infty}{V_\infty}\right] + \frac{\delta\cos\phi}{\cos\phi}$$

$$\left.\frac{\delta B}{B}\right|_r = \frac{\delta\cos\phi}{\cos\phi} = -\tan\phi\ \delta\phi$$

$$\left|\left.\frac{\delta B}{\delta\phi}\right|_r\right| = B\tan\phi$$

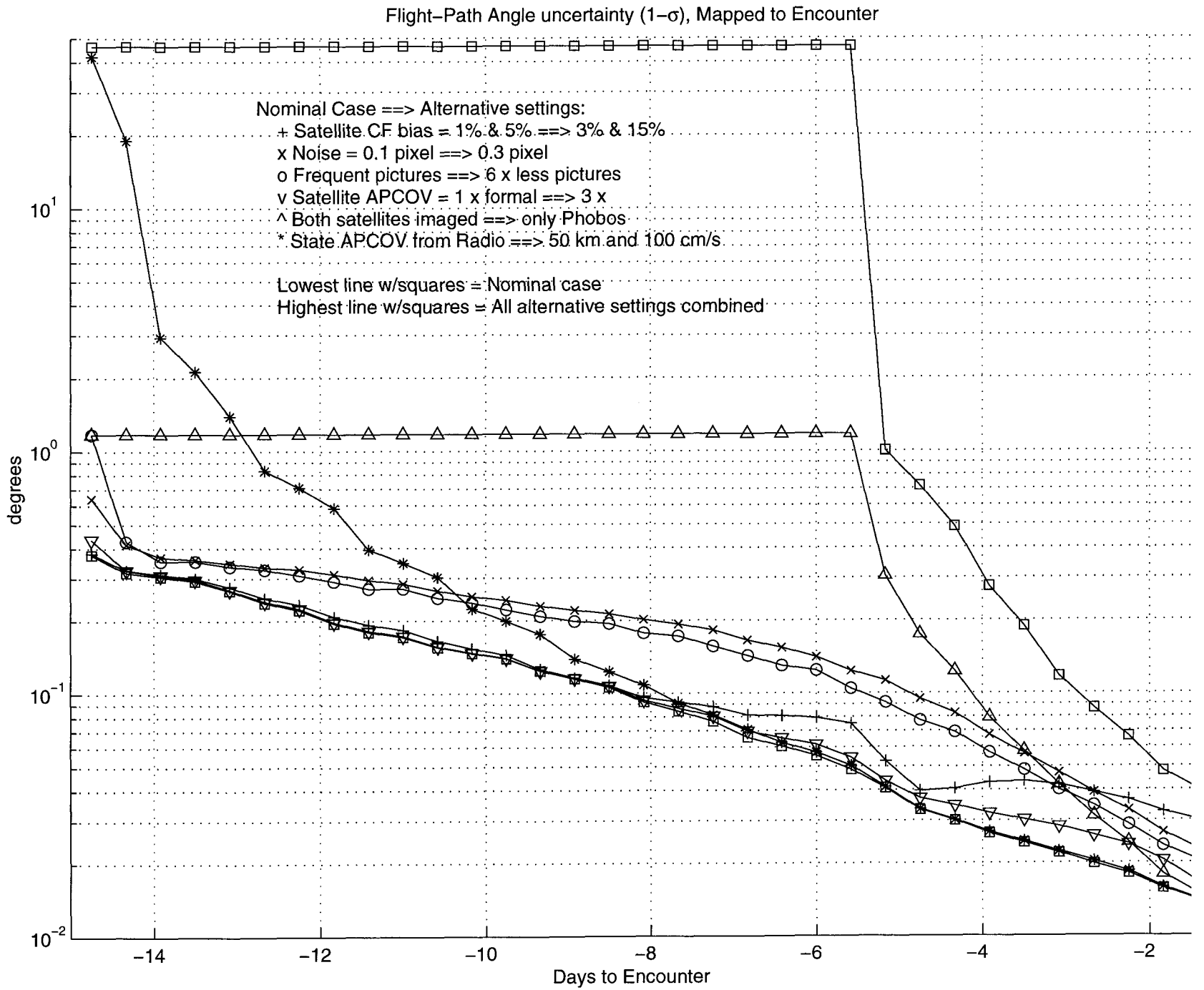
Flight–Path Angle uncertainty (1–σ), Mapped to Encounter
Nominal Case ==> Alternative settings:
+ Satellite CF bias = 1% & 5% ==> 3% & 15%
x Noise = 0.1 pixel ==> 0.3 pixel
o Frequent pictures ==> 6 x less pictures
v Satellite APCOV = 1 x formal ==> 3 x
^ Both satellites imaged ==> only Phobos
* State APCOV from Radio ==> 50 km and 100 cm/s
Lowest line w/squares = Nominal case
Highest line w/squares = All alternative settings combined
degrees
10^{1}
10^{0}
10^{-1}
10^{-2}
−14
−12
−10
−8
−6
−4
−2
Days to Encounter

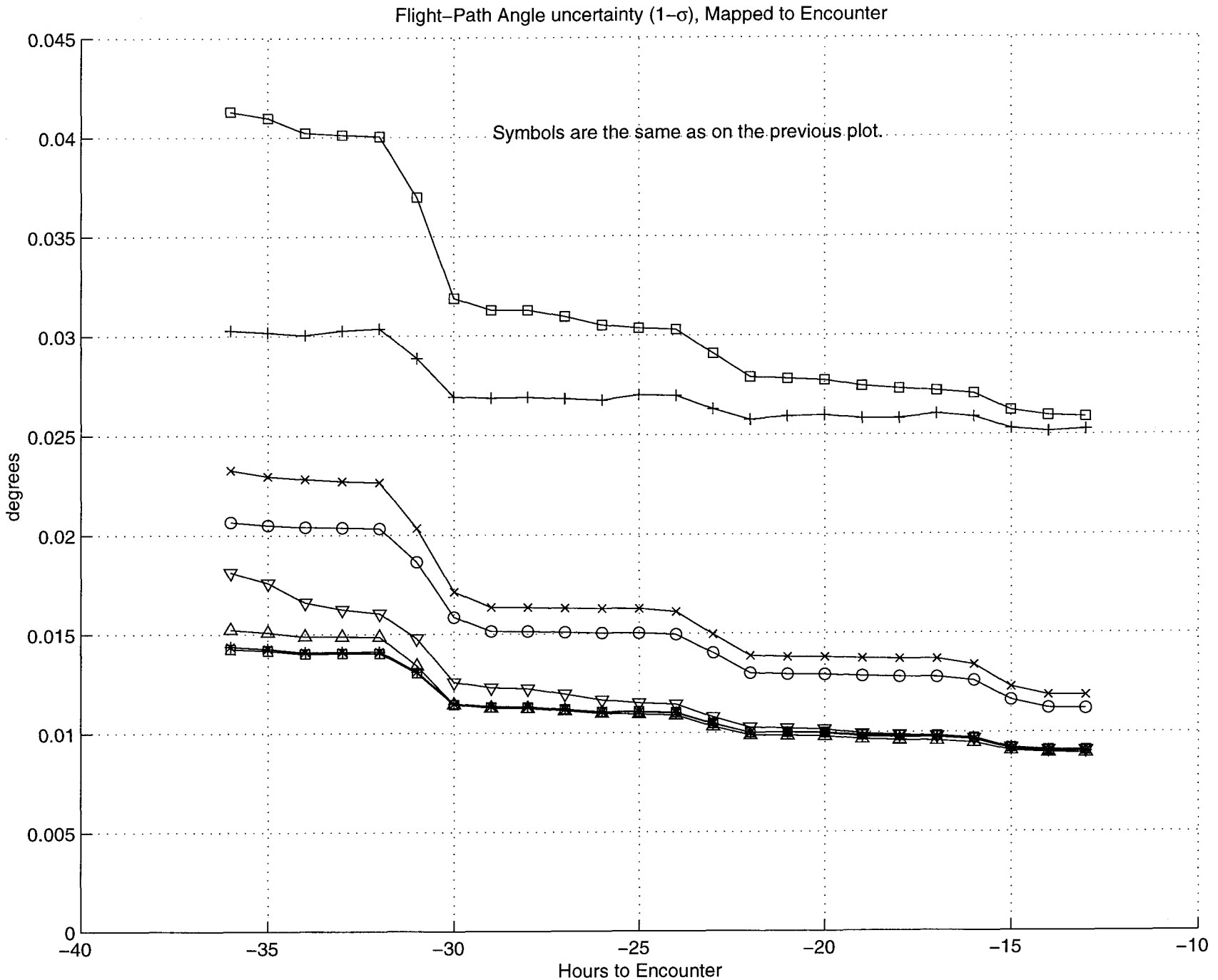
Flight–Path Angle uncertainty (1–σ), Mapped to Encounter
Symbols are the same as on the previous plot.
degrees
Hours to Encounter
0.045
0.04
0.035
0.03
0.025
0.02
0.015
0.01
0.005
0
−40
−35
−30
−25
−20
−15
−10

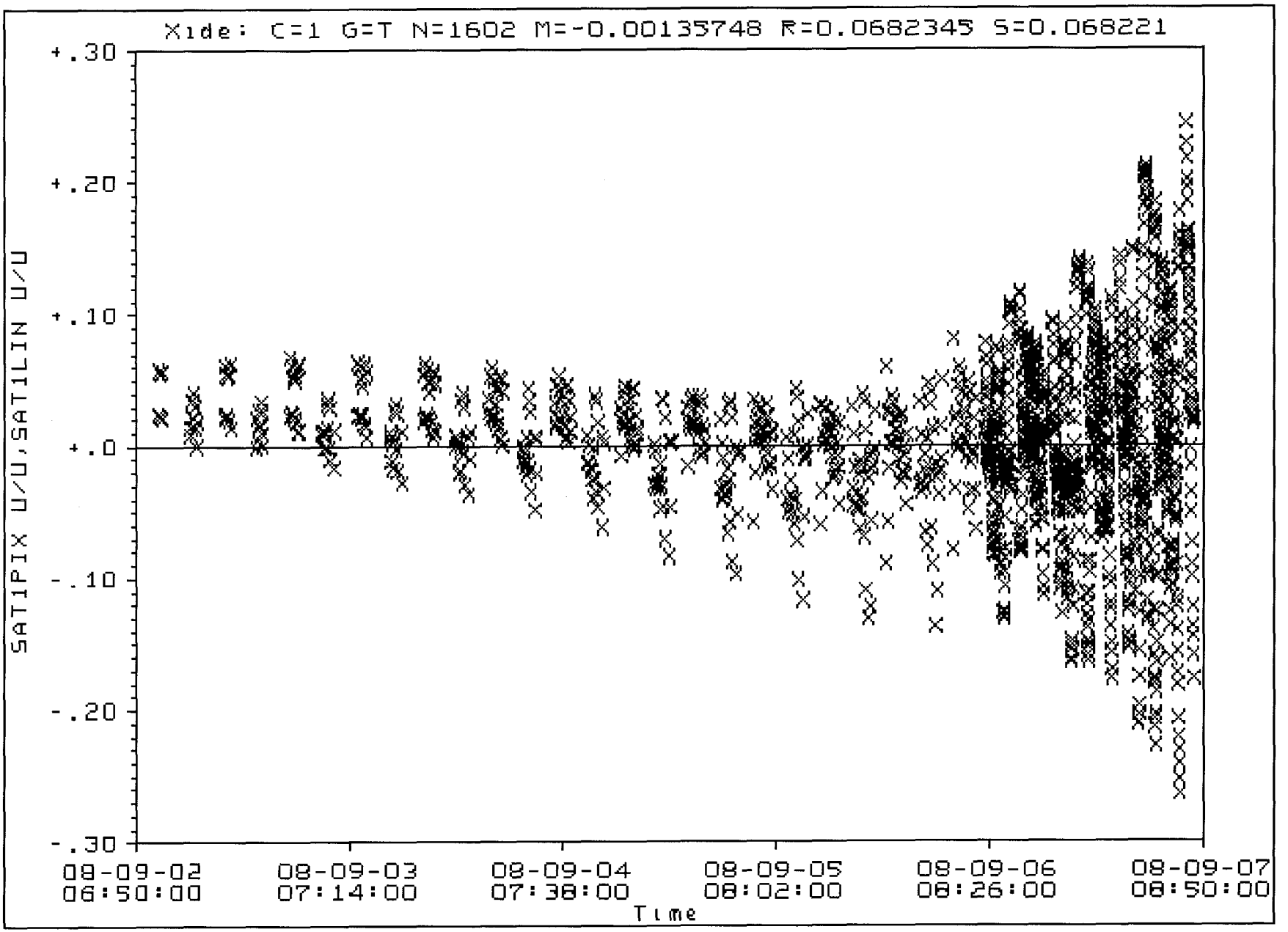
Xide: C=1 G=T N=1602 M=-0.00135748 R=0.0682345 S=0.068221
+.30
+.20
+.10
+.0
-.10
-.20
-.30
SAT1PIX U/U,SAT1LIN U/U
08-09-02 06:50:00
08-09-03 07:14:00
08-09-04 07:38:00
08-09-05 08:02:00
08-09-06 08:26:00
08-09-07 08:50:00
Time

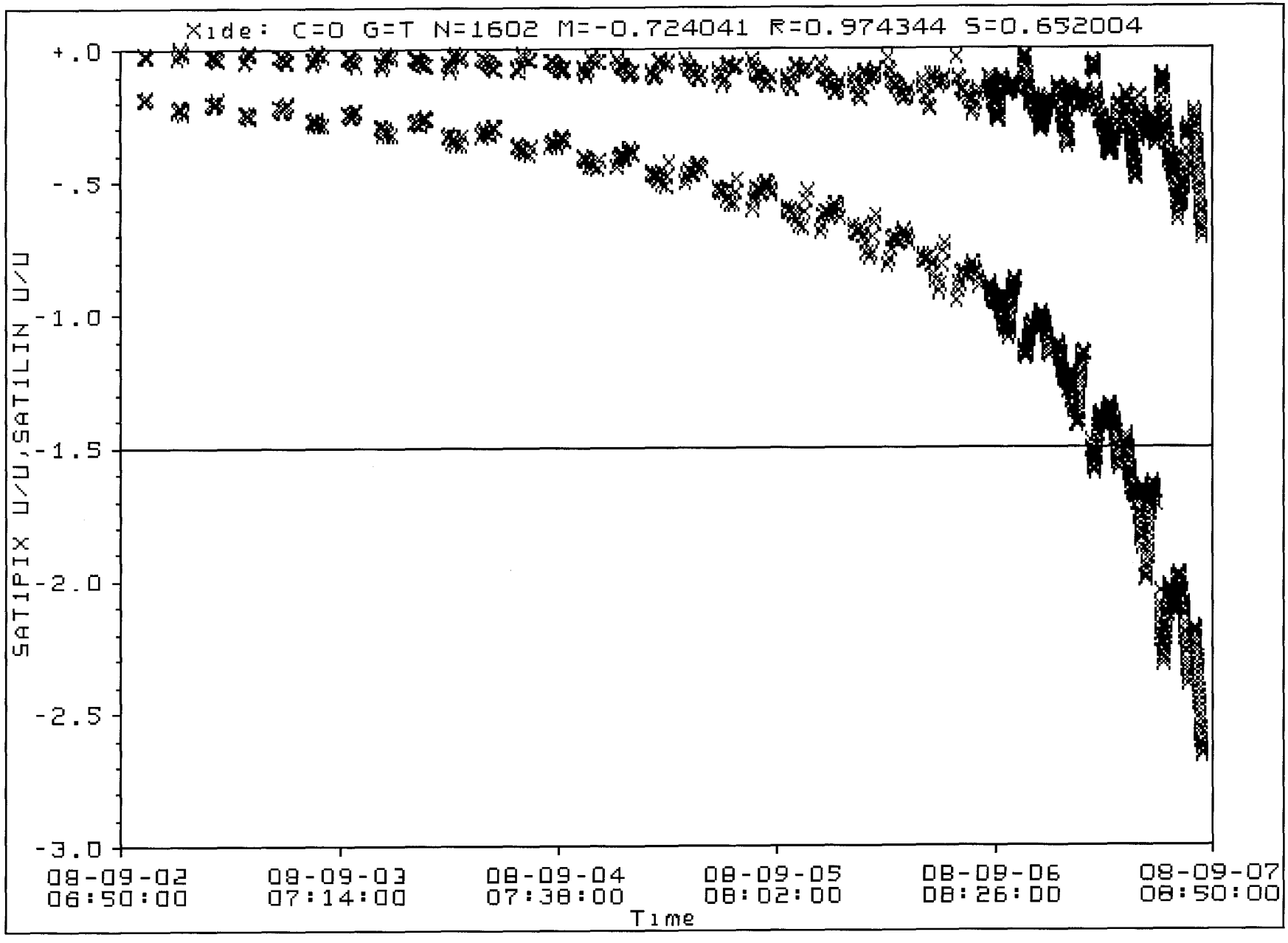
Xide: C=0 G=T N=1602 M=-0.724041 R=0.974344 S=0.652004
+.0
-.5
-1.0
-1.5
-2.0
-2.5
-3.0
SAT1PIX U/U,SAT1LIN U/U
08-09-02 06:50:00
08-09-03 07:14:00
08-09-04 07:38:00
08-09-05 08:02:00
08-09-06 08:26:00
08-09-07 08:50:00
Time

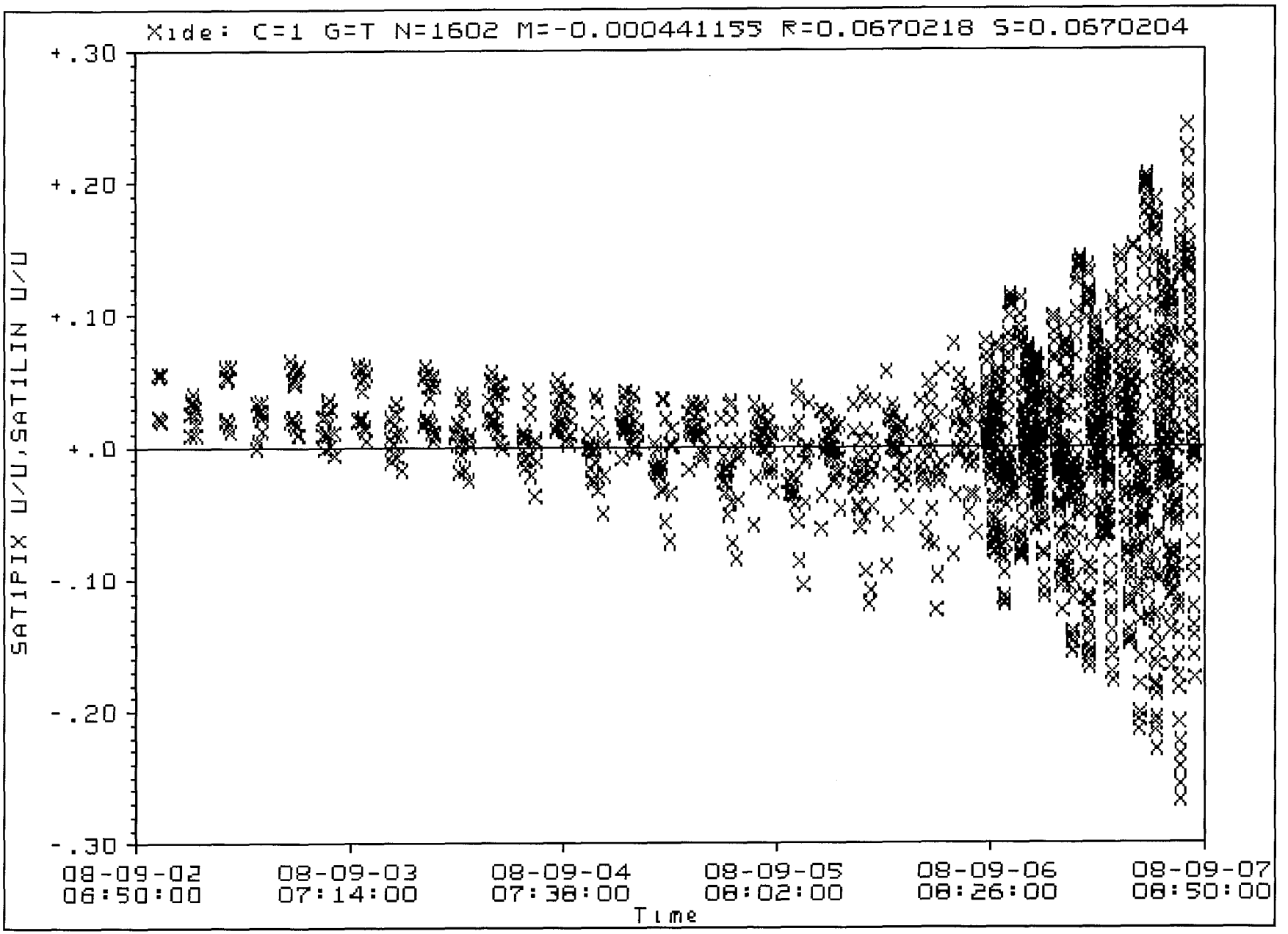
Xide: C=1 G=T N=1602 M=-0.000441155 R=0.0670218 S=0.0670204
+.30
+.20
+.10
+.0
-.10
-.20
-.30
SATIPIX U/U,SATILIN U/U
08-09-02 06:50:00
08-09-03 07:14:00
08-09-04 07:38:00
08-09-05 08:02:00
08-09-06 08:26:00
08-09-07 08:50:00
Time

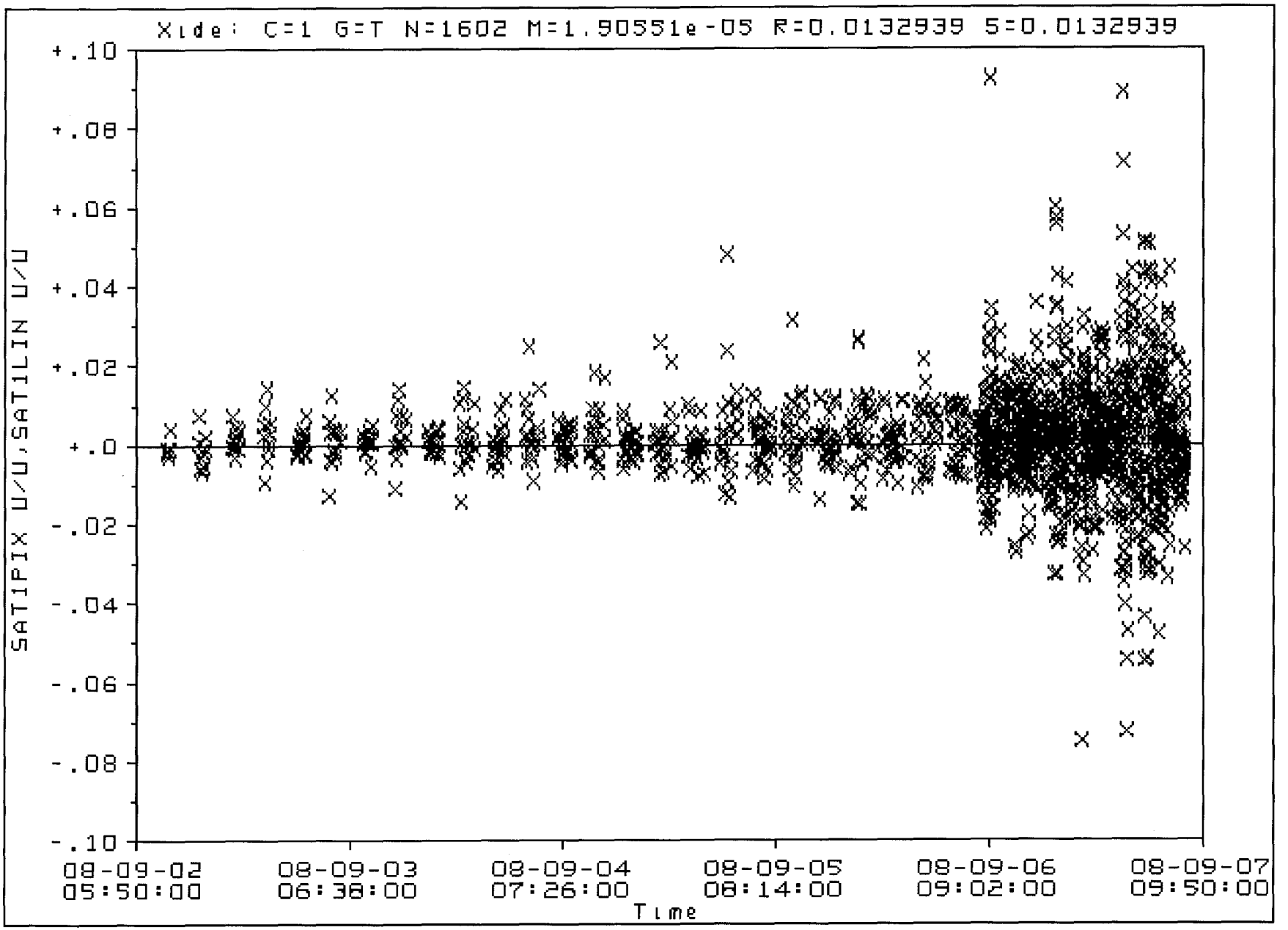
Xide: C=1 G=T N=1602 M=1.90551e-05 R=0.0132939 S=0.0132939
+.10
+.08
+.06
+.04
+.02
+.0
-.02
-.04
-.06
-.08
-.10
SATIPIX U/U,SATILIN U/U
08-09-02 05:50:00
08-09-03 06:38:00
08-09-04 07:26:00
08-09-05 08:14:00
08-09-06 09:02:00
08-09-07 09:50:00
Time

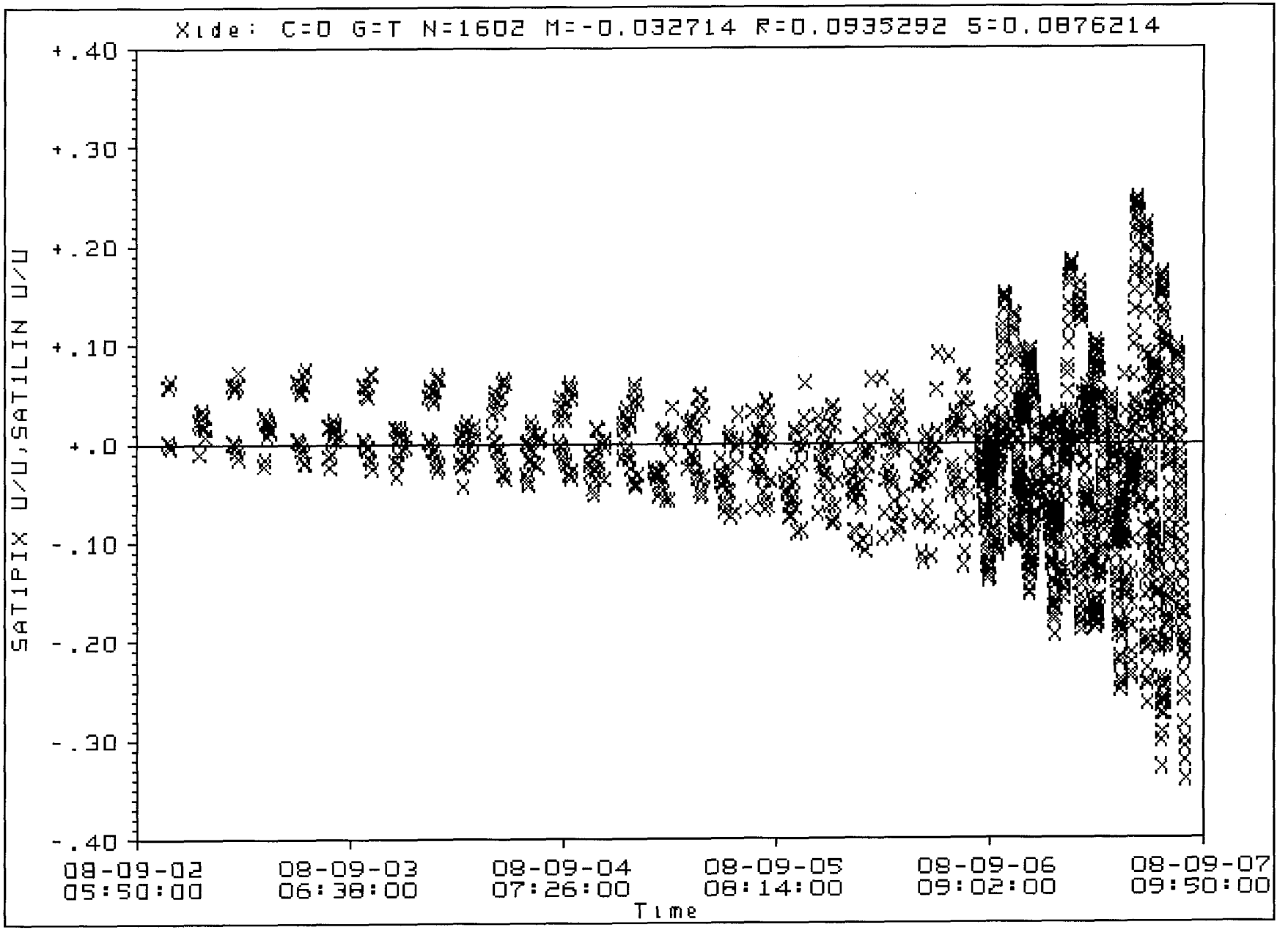
Xide: C=0 G=T N=1602 M=-0.032714 R=0.0935292 S=0.0876214
+.40
+.30
+.20
+.10
+.0
-.10
-.20
-.30
-.40
SATIPIX U/U,SAT1LIN U/U
08-09-02 05:50:00
08-09-03 06:38:00
08-09-04 07:26:00
08-09-05 08:14:00
08-09-06 09:02:00
08-09-07 09:50:00
Time

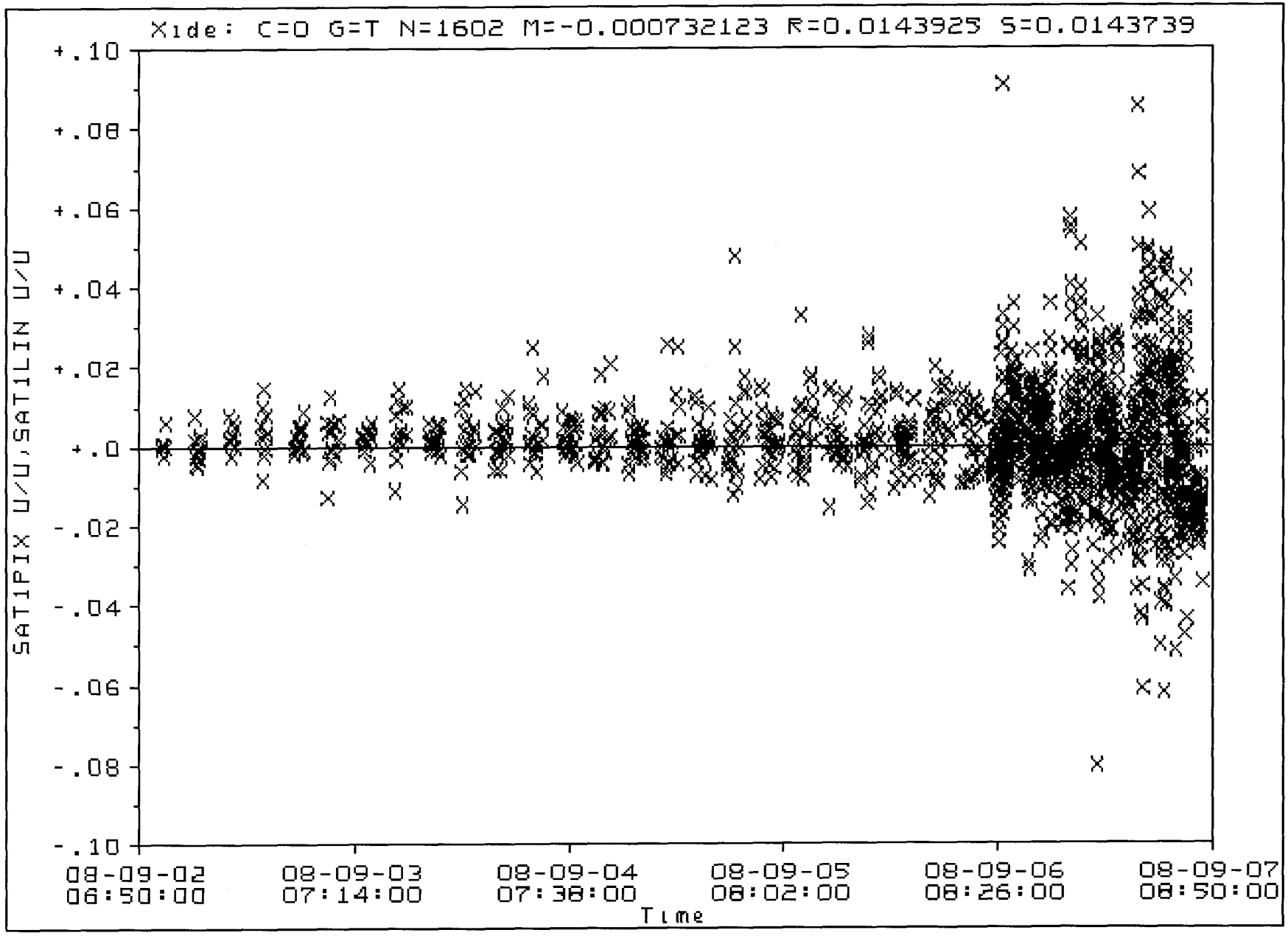
Xide: C=O G=T N=1602 M=-0.000732123 R=0.0143925 S=0.0143739
+.10
+.08
+.06
+.04
+.02
+.0
-.02
-.04
-.06
-.08
-.10
SAT1PIX U/U,SAT1LIN U/U
08-09-02 06:50:00
08-09-03 07:14:00
08-09-04 07:38:00
08-09-05 08:02:00
08-09-06 08:26:00
08-09-07 08:50:00
Time